Tubular Structures XIII – Young (ed)
© 2010 The University of Hong Kong, ISBN 978-0-415-58473-9

Influence of welding residual stresses on stable crack growth in tubular K-joints under compressive fatigue loadings

C. Acevedo & A. Nussbaumer
ICOM-EPFL, Lausanne, Switzerland

ABSTRACT: Tubular bridge design has to deal with fatigue issues. The fatigue susceptibility of these bridges, composed of circular hollow section profiles welded together in K-joints, is mainly due to stress concentrations, to welding imperfections and to tensile residual stresses induced by the welding process.

Since these residual stresses are unknown for K-joints, measurements were carried out in vicinity of weld toes using the incremental hole-drilling method, X-ray diffraction and neutron diffraction in particular. Results from these techniques show that on the first millimeters from the surface, the most important tensile residual stresses are oriented perpendicular to the weld and reach the yield strength. According to experimental investigations on two large scale specimens, it is established that tensile residual stresses have a strong influence down to a depth of 2–3 mm from the surface, allowing cracks to propagate in compressive joints. Preliminary Finite Element Analyses are presented in this paper.

1 INTRODUCTION

Steel tubular truss bridges are composed of circular hollow section members cut and welded together to form the main truss. In order to facilitate welding in the connections between horizontal chords and brace members, overlapping of brace members is often avoided by creating a gap region. These gap K-joints (for truss beams) or KK-joints (for tridimensional structures) are particular to tubular bridge and offshore structures. As explained below, this geometry is especially critical for fatigue strength.

Residual stresses are internal self-balanced stresses introduced in structures or components by local plastic deformation during different manufacturing processes such as welding. Since tensile residual stresses tend to open cracks, they have a detrimental influence on the fatigue crack propagating under cyclic traffic loadings on the bridge. In tubular K-joints, the welding process creates high tensile residual stresses in the gap between the braces, with a magnitude reaching the yield strength of the steel (355 MPa for the steel of grade S355 commonly used in steel bridges).

This study focuses on joints loaded under compression (upper chord joints), where tensile residual stress effect on fatigue life can be set apart from external loads effect. With welding imperfections acting like microcracks, residual stress can make the difference between a fatigue microcrack beginning to grow or not (McClung, 2006). Indeed, residual stress can raise the effective stress intensity factor range above the threshold ΔK value. Moreover, it also influences the rate of crack propagation, since the tensile residual stress field is often associated with shorter fatigue life. Therefore, the residual stress distribution is essential to estimate accurately the crack development under fatigue loads. However, to the best of our knowledge, no data are available concerning residual stress investigations in K-joints used in bridge construction.

In this work, results of residual stress measurements are presented and a distribution function is proposed for the critical transverse residual stress field in the weld toe vicinity. Based on this distribution, Linear Elastic Fracture Mechanics can be used to estimate the fatigue crack growth in K-joints loaded under compression. Finally, this model was validated with the results from large scale fatigue test.

2 LEFM FATIGUE MODEL

Linear Elastic Fracture Mechanics (LEFM) has proven to be a useful analytical tool to estimate the behavior of cracks in solids in order to evaluate the critical loads that cause crack growth. In this study, fracture under mode I (the opening mode) is assumed, which is the most probable for metallic structures. For isotropic linear elastic materials, the concept of the stress intensity factor K has been introduced by Irwin (1957) in order to characterize,

with this single parameter, the local stress field near the crack tip. The stress intensity factor K for an elliptical crack can be expressed as follows:

$$K = Y \cdot \sigma \cdot \sqrt{\pi \cdot a} \tag{1}$$

where Y is the correction factor for various effects (shape of the crack, presence of free surface, thickness of the plate and non-uniformity of stress distribution); σ is the stress; and a is the crack size.

It has to be noticed that, since the crack size a is a term of the expression, it is assumed that an initial crack is present in the material (which is often true with crack-like imperfections induced by welding) implying that no initiation stage is considered.

In combination with the LEFM, the well-known Paris law is used in order to predict the stable crack growth under fatigue loadings (Paris & Erdogan (1963)):

$$\frac{da}{dN} = C \cdot \Delta K_{app}{}^{m}$$
$$\Delta K_{app} = K_{app,max} - K_{app,min} \tag{2}$$

where da/dN is the propagation rate (N is the number of cycles); C and m are constants of the material; and ΔK_{app} is the applied stress intensity factor range ($K_{app,max}$ is related to the applied maximum load and $K_{app,min}$ to the applied minimum load).

Modifications of Equation (2) can be done to take into account the threshold stress intensity factor range, ΔK_{th}, under which no propagation can occur.

$$\frac{da}{dN} = C \cdot (\Delta K_{app} - \Delta K_{th})^{m} \tag{3}$$

To consider the residual stress field and the crack tip plasticity into the LEFM fatigue approach, Bremen (1989) has shown that the principle of superposition can be used to calculate the effective stress intensity factor, K_{eff}.

As shown by Elber (1970), a fatigue crack can remain closed at the crack tip for a portion of the tensile load cycle, meaning that only a part of the cycle is effective in propagating the crack. Indeed, behind the crack tip, tensile deformations are left along crack faces from all previous plastic zones. These deformations come with a shortening of the crack opening displacement, explaining why the crack tip may be closed for tensile load greater than zero.

Hence, K_{op}, defined as the applied stress intensity factor level above which the crack tip opens upon loading, is related to the crack tip plasticity K_{pl}. In the absence of residual stress, $K_{op} = -K_{pl}$.

However, residual stresses influence also the crack tip opening or closure. Tensile residual stresses, induced by the welding process, tend to open crack faces whereas compressive residual stresses, induced by post-treatment methods, tend to close the crack. The influence of the residual stress distribution can be considered with K_{op}: $K_{op} = -(K_{res} + K_{pl})$.

The concept of K_{eff} is based on the following expression:

$$K_{eff} = K_{app} + K_{res} + K_{pl} = K_{app} - K_{op} \tag{4}$$

Bremen (1989) proposed the following relation for ΔK_{eff}, resulting in Equation (6).

$$\Delta K_{eff} = MAX(K_{app,max} - K_{op}, 0) - MAX(K_{app,min} - K_{op}, 0) \tag{5}$$

Then the crack closure method is adopted by replacing ΔK_{app} in Equation (3) by the effective ΔK_{eff}.

$$\frac{da}{dN} = C \cdot (\Delta K_{eff} - \Delta K_{th})^{m} \tag{6}$$

The principle of superposition in Equation (4) is based on the assumption that the stress distribution is not affected by the presence of a crack. Based on this assumption, one can calculate K_{res} by making use of the correction factors proposed by Albrecht & Yamada (1977) and K_{app} by direct calculation of Bowness & Lee (1999).

Contrary to other fatigue design approaches for tubular joints, such as the classification method (EN1990, 2002) or the hot-spot stress method (IIW, 2005), LEFM allows to estimate the crack size and the crack growth rate during the service life of a structure.

3 RESIDUAL STRESS MEASUREMENTS

3.1 *Neutron diffraction measurements*

Since neutron beam can penetrate deeply in the sample without changing the atomic lattice of the material, it is much preferred to X-ray and Hole-drilling techniques.

Neutron diffraction provides the residual stress distribution in three dimensions for depth up to 15 mm.

Three series of neutron diffraction measurement were conducted on different samples. During the first one, carried out at the Paul Scherrer Insitute PSI (Villigen, Switzerland), an as-welded

(untested) K-joint with a chord wall thickness of 30 mm was investigated. The second series was carried out at the Institute Laue-Langevin ILL (Grenoble, France) on a fatigue-tested K-joint sample with a chord wall thickness of 20 mm. The last series was performed in PSI on a fatigue-tested K-joint sample with a chord wall thickness of 30 mm. Fatigue-tested samples are non-cracked K-joints cut from the tubular truss beams tested under fatigue (see section 4). Samples were all composed of part of the chord with two brace member parts welded onto it (see Figure 1).

Residual strains were obtained from the measurement of the lattice strain on the 211 reflection plane, with gauge volumes of respectively $2\times2\times2.5\,mm^3$, $2\times2\times2\,mm^3$ and $3.8\times3.8\times3.8\,mm^3$ for the first, second and third series.

In order to identify a possible peak stress relaxation and redistribution during the first fatigue cycles, strains at different positions underneath the weld toe from the as-welded (1st series at PSI) and fatigue-tested (3rd series at PSI) samples are compared in Figure 2.

Since only radial strains were obtained from the first series, comparisons are based on this strain direction. It can be seen on this figure that indeed some relaxation of the radial strain field occurs on the first 4 mm, resulting in a redistribution of strain magnitude along the depth in the chord wall thickness. However, one cannot extend this conclusion to radial and longitudinal strains even if this shake-down effect is often encountered for high-cycle fatigue with high stress range.

A study concerning the influence of the sample thickness on the residual stress distribution has also been conducted to identify if the residual stress distribution function is best related to z/T or to z (where z is the depth below the surface of chord wall and T the chord wall thickness). Comparison between neutron diffraction transverse strains in the weld toe vicinity, for a chord wall thickness of 20 mm (2nd series at ILL) and of 30 mm (3rd series at PSI) is presented in Figure 3.

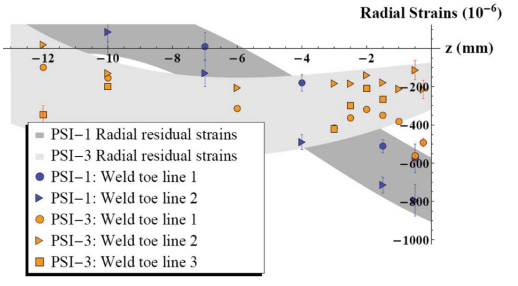

Figure 2. Radial residual strains measurement points and envelopes for the as-welded sample (PSI-1) and the fatigue-tested sample (PSI-3) with chord wall thicknesses of 30 mm.

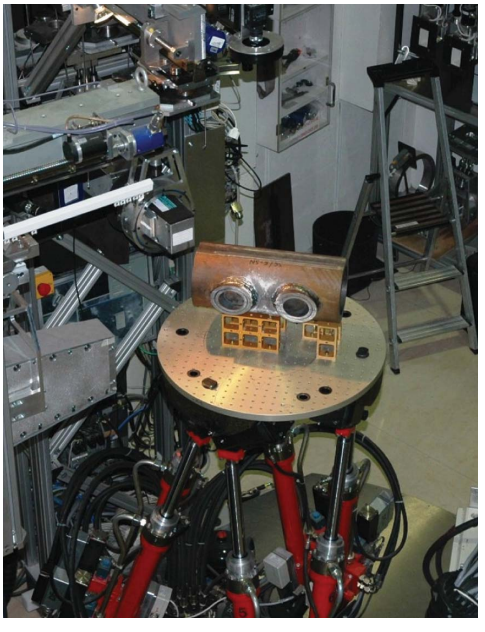

Figure 1. K-joint sample during transverse residual strain measurements at ILL (2nd series).

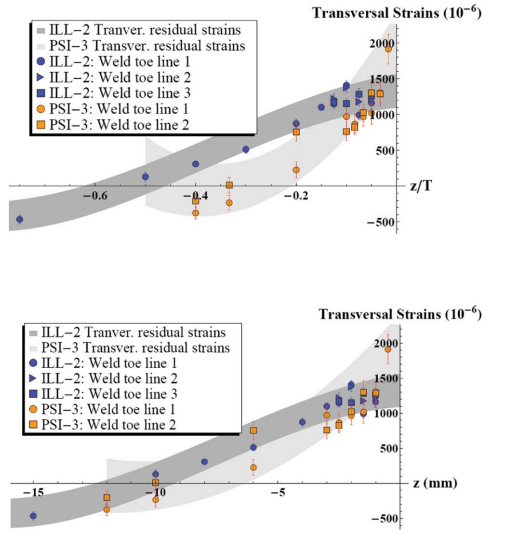

Figure 3. Transverse residual strains measurement points and envelopes for the fatigue-tested samples with a chord wall thickness of 20 mm (ILL-2) and a chord wall thickness of 30 mm (PSI-3), respectively.

It seems that the transverse strain distribution is better related to z than to z/T. Since the transverse strain distributions versus depth z are quite similar for a 20 mm or a 30 mm thick wall, it can be considered as a non-proportional size-effect, even if distributions are not perfectly superimposed and even if this trend is not so clear for longitudinal and radial strains.

Based on these considerations, the second or the third series of measurement can be chosen to estimate the residual stress distribution. Since more data points are available from the measurements at ILL, these results are presented in more detail below. Residual stress mappings deduced from measurements are depicted in Figure 4. The transverse direction is perpendicular to the weld, the

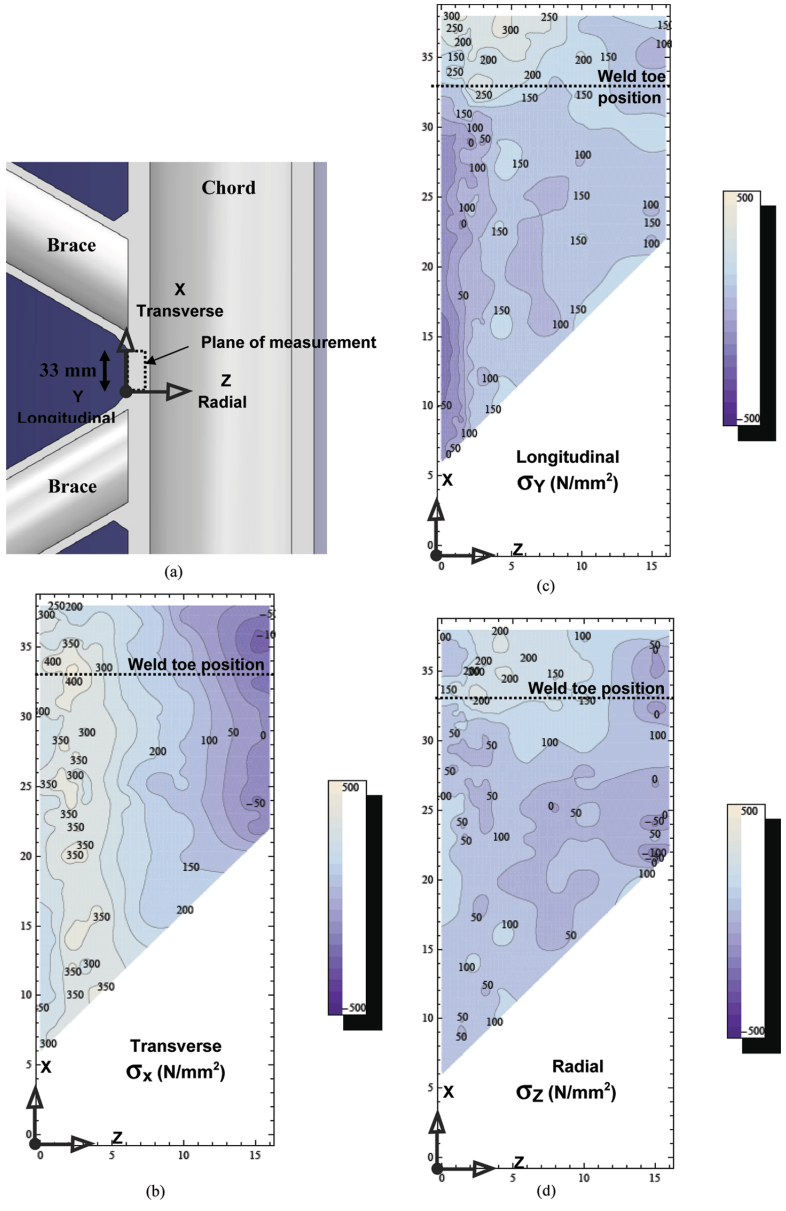

Figure 4. Residual stress mappings from the 2nd serie (ILL). (a) Plane of measurement (b) transverse direction (c) longitudinal direction (d) radial direction.

longitudinal direction is parallel to the weld and the radial direction is the depth direction. Points of measurements were taken along the longitudinal tube axis, along a line in the gap between the two welds and depth scans were made (see plane of measurement in Figure 4). A thousand points were used to draw these plots.

Figure 4 shows that, tensile transverse residual stresses reach the yield stress value in the area around the weld toe and are greater than longitudinal ones, which is not the case for tubular butt welds. Moreover, this particular orientation of the largest residual stresses is also the orientation of the externally applied stresses, as a consequence they will superimpose in a detrimental way. On top of that, the magnitude of the transverse residual stress remains high in the gap region due to a restraining effect between braces. This effect induces tensile residual stresses over most of the wall thickness and in the whole gap region. Note that these residual stresses are not self-equilibrated since we look only at a local region.

The geometry of the K-joint is responsible for both high applied stresses as well as, due to welding, high residual stresses in the same region, which is critical for fatigue.

3.2 *Hole-drilling and X-ray measurements*

The hole-drilling and X-ray methods were also used to evaluate the magnitude of transverse and longitudinal residual stresses in the surface.

Because of the complex geometry of the K-joints, a drilling device had to be designed and built in our laboratory. The instrumentation and calibration tests carried out to validate the method are described in more detail in Acevedo (2009a). Data points presented in Figure 5 were obtained at a 2 mm depth for different sample thicknesses, which were either as-welded or fatigue-tested.

X-ray measurements were performed at IFS (Braunschweig University, Germany) on the 30 mm thick as-welded sample previously tested at PSI (1st series). Neutron diffraction points drawn in this figure were measured at a depth of 2 mm.

In Figure 5, comparison of transverse and longitudinal stresses along the axial line in the gap does not show a good agreement between the three techniques. This discrepancy is partially explained as follows.

First of all, hole-drilling values seem to be higher than others especially in the weld vicinity region where residual stress reaches the value of the yield stress. However, it is well known that if residual stresses exceed 60% of the material yield stress, the accuracy of the hole-drilling measurement will decrease, explaining why values deduced from hole-drilling are even greater than 400 N/mm^2.

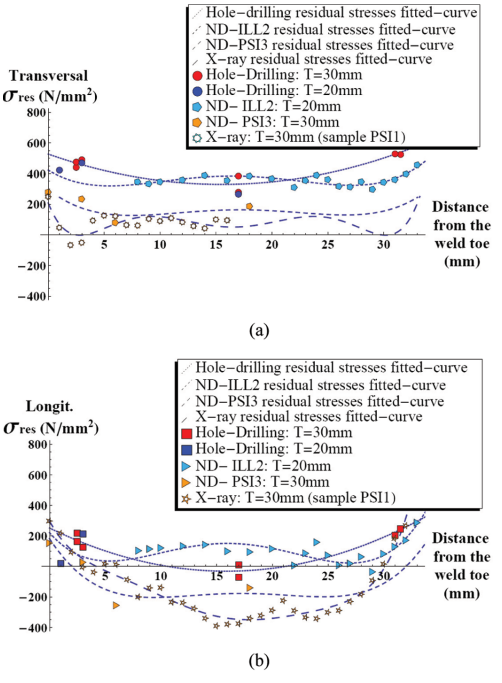

Figure 5. Comparison of residual stress distribution (hole-drilling, neutron diffraction and X-ray) along the axial line in the gap knowing that weld toes are situated at 0 and ~33 mm. (a) Transverse direction (b) Longitudinal direction.

Concerning neutron-diffraction investigations, although few values are available for the 3rd series at PSI, one can argue that data points are shifted by approximately 200 N/mm^2 compared to the 2nd series, highlighting the fact that the residual stress magnitudes are quite different especially on the first millimeters (see Figure 3). At this step of the study and making reference to Figure 3, it is difficult to link these results with a possible size effect.

Finally, X-ray values show some similarity with neutron diffraction values for the sample of the same thickness. Transverse neutron diffraction values are greater than X-ray values in the same direction whereas it is the opposite in the longitudinal direction, implying that no real shake-down effect can be identified from this comparison.

3.3 *Profile of distribution for transverse residual stresses*

As mentioned above, transverse residual stresses are of most interest for fatigue assessment since they superimpose with principal applied stresses.

Assuming from Figure 3 that a distribution function related to z is the suitable way to characterize

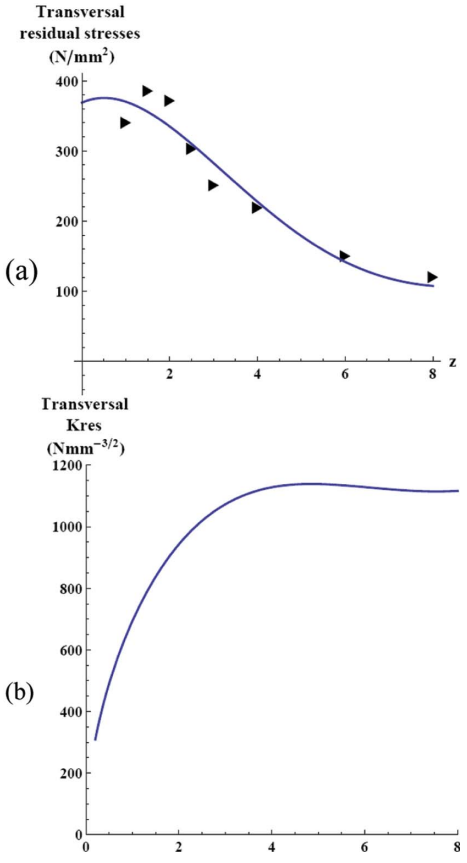

Figure 6. Transverse residual stress (a) distribution (b) stress intensity factor.

transverse residual stresses, a distribution shown in Figure 6 is proposed (where z is the vertical distance below the surface). Since this function will be used further to calculate the stress intensity factor in a compression joint with a 20 mm thick chord wall, the curve was fitted to the ILL measurement points. Transverse stresses are projected along a plane inclined by 60° with the vertical plane in order to approximately reproduce the transverse stress field along the real crack plane.

The stress intensity factor K_{res} based on this distribution and calculated using Equation (1) is depicted in Figure 6(b).

4 APPLICATION OF LEFM MODEL AND COMPARISON WITH A FATIGUE TEST

4.1 *Description of fatigue tests*

Two fatigue tests were carried out in our laboratory on large scale tubular truss beams. Each truss was composed of one upper chord (Circular Hollow Sections ROR 168.3 × 30 resp. 20 mm) of approximately 9 m long, one lower chord (ROR 168.3 × 20 resp. 30 mm) of approximately 7 m long and six braces connected to the chords. A fatigue load Q (Q_{max} = 610 kN, Q_{min} = 60 kN) was applied at the mid-span on the truss which was supported at both ends of the upper chord. More information concerning the test setup and the test results are presented in Acevedo (2009b).

Each specimen was composed of seven tubular K-joints, all of which were partially or totally cracked at the end of the test except the joint located at the actuator position, which had previously been post-weld treated for security reasons. All cracks occurred in the gap at the weld toe positions, on the tension side as well as on the compression side, mainly explained by the combination of stress concentrations, weld toe imperfections and high tensile residual stresses.

The compressive K-joint of interest was equipped with an Alternative Current Potential Drop, ACPD, in order to monitor the crack growth during the fatigue tests. This joint is situated on the chord loaded under compression with one brace in tension and one in compression. Three pairs of probes were located on the tensile brace toe and five pairs on the compressive brace weld toe. The crack depth was recorded and used to derive the crack propagation rate and the stress intensity factor.

4.2 *Comparison of stress intensity factors*

Using the fracture mechanics fatigue model developed in Section 2, the applied SIF range, ΔK_{app}, is calculated using the Bowness & Lee (1999) formulation based on Q_{max} and Q_{min} values. The opening SIF K_{op} is obtained from K_{res} (Section 4.1) and from K_{pl}. The threshold SIF range, ΔK_{th}, is expressed as follows (Zheng, 1987): $\Delta K_{th} = 320 \cdot (1\text{-}R)$ and is equal to 288 N/mm$^{3/2}$ with R = 0.1.

Then the effective SIF range can be deduced from Equation (5). Figure 7 combines the SIF range obtained from ACPD measurements and from the fracture mechanics model.

It appears that in both cases, under compressive and tensile applied stresses, the effective ΔK_{eff} is positive explaining why cracks propagate on both sides. A positive ΔK_{eff} in a joint loaded under compression is only possible because $K_{op} < K_{app,max} < 0$ whereas in the absence of residual stresses $K_{op} > K_{app,max}$. Indeed, the more positive K_{res} is, the more negative K_{op} is. In a special K-joint geometry with high tensile residual stresses and restraining effects, K_{res} remains high for important crack depths, implying that K_{op} remains highly negative, although, not high enough to keep the entire

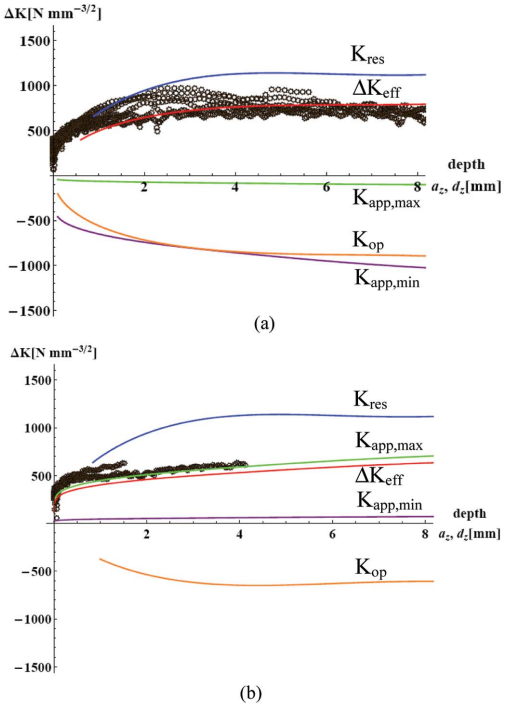

Figure 7. Comparison of Stress intensity factors between fatigue test values and LEFM fatigue model curves (a) on the compressive brace side (b) on the tensile brace side.

cycle effective for crack propagation ($\Delta K_{eff} < \Delta K$). Therefore, the crack propagation rate is run by $\Delta K_{eff} = K_{app,max} - K_{op}$.

To summarize, in joints loaded under compression, tensile residual stress distribution has a strong influence on magnitude and shape of ΔK_{eff}, and finally ΔK_{eff} deduced from LEFM is a convenient tool to estimate if crack will propagate faster, slower or just stop.

On the other side, in joints loaded under tension, since K_{op} is usually lower than $K_{app,min}$, $\Delta K_{eff} = \Delta K_{app}$ with or without presence of tensile residual stresses.

5 FINITE ELEMENT MODELS

5.1 *Profile of distribution for transverse residual stresses*

A three-dimensional Finite Element Analysis FEA was performed in ABAQUS/standard 6.9 to simulate the MAG-welding process in order to get the residual stress distribution. To do so, an uncoupled thermo-mechanical analysis is used in a similar manner as described by Drez et al. (2006) for laser beam welding of butt joints of aluminum alloys.

Modeling of stress build-up during welding is a high complex problem (Lindgren, 2001). Indeed, temperature dependent thermal and mechanical properties for each material (base material and weld material) must be defined from room temperature up to the melting temperature. Since phase transformation takes place at high temperatures, mechanical characteristics for each phase (ferrite-pearlite, austenite, martensite, bainite) should also be known. In multi-pass welding, metal deposition for each pass has to be considered together with annealing induced by melting-remelting.

Some simplifications were made in the FEA. Multi-pass welding was simulated as a single pass with an equivalent heat source. This heat source is composed of a volumetric flux moving around the weld line at the welding speed. The characteristics of the heat source are determined so that the computed size of the weld pool matches the one measured on a macrograph. Metal deposition is not considered, the finite elements representing the weld are present in the model from the beginning.

Moreover, according to Dong & Hong (2002), phase transformation can be neglected for carbon steel due to the fact that martensite transformation is localized around the Heat Affected Zone and induces small residual stress variations.

The thermal analysis was formulated in terms of heat conduction, heat losses by radiation and convection and heat input simulating the welding source. Latent heat of fusion was also included.

Since fluid flow was not considered, an artificial increase of thermal conductivity was introduced above the solid-liquid temperature.

The second step consists in imposing the thermal field determined in the first step in an elasto-plastic mechanical analysis. The plastic deformations in the

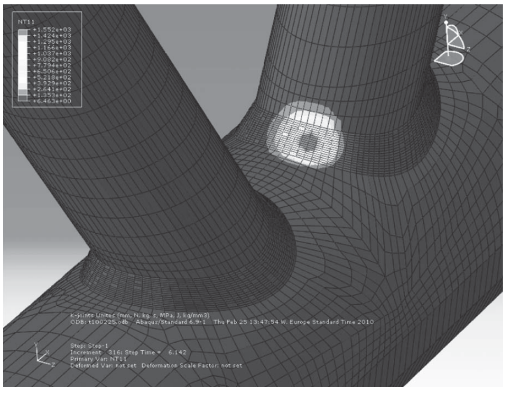

Figure 8. Temperature output obtained with the thermal model.

liquid state are reset to zero using the *ANNEAL TEMPERATURE function in Abaqus.

5.2 *Crack propagation analysis*

In future work, applied stresses will be added to the residual stress field, and an eXtended Finite Element Model XFEM will be employed to propagate a crack without remeshing. Since the mesh is generated independent of a crack in this technique, it allows the crack to propagate in an arbitrary path. This aspect is important in our case because the crack path can drastically change with the geometrical dimensions of the K-joints.

This method will be used to validate the change of the crack shapes in our two fatigue tests and to identify parameters (geometrical dimensions, residual stress distribution, applied stress distribution …) inducing this effect.

6 CONCLUSION

Residual stress measurements were carried out on welded tubular K-joints using neutron diffraction, hole-drilling and X-ray. A LEFM fatigue model, derived from Paris law, was applied on a K-joint loaded under compression to estimate the effective stress intensity factor range at the weld toe between braces. This model used the residual stress distribution obtained with neutron diffraction measurements. The calculated ΔK_{eff} was compared with the stress intensity factor range deduced from fatigue test measurements. The main objective was to study the influence of tensile residual stresses induced by welding on fatigue crack growth in compressive joint. Major conclusions are summarized as follows:

- The LEFM was in good agreement with measurement results. This method is a useful tool to estimate ΔK_{eff} and the rate of propagation. The assumption, that the stress distribution is not affected by the presence of a crack, seems to be acceptable. The transverse residual stress distribution proposed from neutron diffraction results has given good results.
- Neutron diffraction is a powerful and reliable method to measure residual stresses. Neutron diffraction allowed identifying a probable shakedown effect. However, it didn't show clearly the existence of a non-proportional size effect. To pursue these investigations, parametric studies on geometrical size effect have to be made using thermo-mechanical FEM.
- The effect of tensile residual stresses in fatigue crack growth of compressive K-joints has been shown by the large scale fatigue tests and by the LEFM model. Tubular K-joints are particularly susceptible to tensile residual stress influence because of the restraining effect in the gap region creating high and extensive tensile residual stresses critically oriented transversely to the weld direction.

ACKNOWLEDGMENTS

This research is part of a PhD project funded by the Swiss National Science Foundation (SNF). The tubes used to build the large scale tubular truss beam specimens were provided by V & M Deutschland GmbH. The specimens were fabricated and welded by Zwahlen & Mayr S.A.

The authors would like to thank Dr. J.M. Drezet from LSMX (EPFL) and Dr. A. Rossoll from LMM (EPFL) for their help and advice concerning the FE modeling.

Thanks are also due to Dr. A. Evans from the Paul Scherrer Institute (POLDI) and Dr. D.J. Hughes from the Institute Laue-Langevin (SALSA) for their know-how in neutron diffraction measurements.

REFERENCES

Acevedo, C. & Nussbaumer, A. 2009a. Residual stress estimation of welded tubular K-joints under fatigue loads. *Proceedings of the 12th International Conference on Fracture ICF12, Ottawa, 12–17 July 2009*.

Acevedo, C. & Nussbaumer, A. 2009b. Study on crack propagation in tubular joints under compressive fatigue loadings. *Proceedings of the International Conference on the respective input of the numerical simulation and the experimental approach in Fatigue Design 2009, Senlis, 25–26 November 2009*.

Albrecht, P. & Yamada, K. 1977. Rapid calculation of stress intensity factors. *Journal of Structural Engineering ASCE* 103(ST2):377–389.

Bowness, D. & Lee, M.M.K. 1999. Weld toe magnification factors for semi-elliptical cracks in T-Butt joints. *Offshore Technology Report-OTO 199 014*. UK: Health and Safety Executive (HSE).

Bremen, U. 1989. *Amélioration du comportement à la fatigue d'assemblages soudés: etude et modélisation de l'effet de contraintes résiduelles*. Lausanne: EPFL Thesis N°787.

Dong, P. & Hong, J.K. 2002. Recommendations for determining residual stresses in fitness-for-service assessment. *Welding Research Council bulletin 476, November 2002*.

Drezet, J.M. & al. 2006. FE modelling of laser beam welding of aluminium alloys with special attention to hot cracking in transient regimes. In H. Cerjak (ed.), *Mathematical Modelling of Weld Phenomena* 8:137–152.

Elber, W. 1970. Fatigue crack closure under cyclic tension. *Engineering Fracture Mechanics* 2(1):37–45.

EN1990, 2002. European Committee for Standardization. *EN1990-Basis of structural design. Brussels, 2002*.

IIW International Institute of Welding, 2005. Recommendations for fatigue design of welded joints and components. *IIW Doc. XIII-1965-03/XV-1127-03, June 2005*.

Irwin, G.R. 1957. Analysis if stresses and strains near the end of a crack traversing a plate. *Journal of Applied Mechanics* 24:361–364.

Lindgren, L.E. 2001. Finite element modeling and simulation of welding, Part 1: Increasing complexity. *Journal of Thermal Stresses* 24*:*141–192.

McClung, R.C. 2006. A literature survey on stability and significance of residual stresses during fatigue. *Fatigue and Fracture of Engineering Materials and Structures* 30:173–205.

Paris, P. & Erdogan, F. 1963. A critical analysis of crack propagation laws. *Transactions of the ASME (Series D)* 85(4):528–534.

Zheng, X. 1987. A simple formula for crack propagation and a new method for the determination of DKth. *Engineering Fracture Mechanics* 27(4):465–475.